GEOPHYSICAL RESEARCH LETTERS, VOL. 16, NO. 9, PAGES 1043-1046, SEPTEMBER 1989

MULTI-TRACE DECONVOLUTION WITH UNKNOWN TRACE SCALE FACTORS: OMNILINEAR INVERSION OF *P* AND *S* WAVES FOR SOURCE TIME FUNCTIONS

Larry J. Ruff

Department of Geological Sciences, University of Michigan

Abstract. Seismic source and wave propagation theories allow seismologists to compute long period synthetic seismograms that commonly match even subtle details of observed waveshapes, but the overall trace amplitudes must be scaled by arbitrary factors to emphasize the excellent waveshape correspondence. This unexplained amplitude scatter causes considerable difficulties when formally inverting observed waveforms for seismic source parameters. Omnilinear inversion simultaneously determines the linear model parameters and trace scaling factors to minimize the mismatch between observed and synthetic seismograms. Omnilinear inversion is applied to source time function deconvolution from long period *P* and *SH* waves. A simulation with synthetic data shows that omnilinear inversion finds the proper scaling factors, and the source time function and focal depth are better determined than for "standard" linear inversion. Omnilinear inversion is then applied to a data set of seven *P* waves and one *SH* wave from the underthrusting earthquake of July 5, 1968 (M_S 6.6) in northern Honshu, Japan. Omnilinear inversion produces a best-fit focal depth of 36 km with a single pulse time function of 6 s duration and seismic moment of 4×10^{18} N m (M_W 6.4). This focal depth supports the notion that the seismically coupled plate interface extends no deeper than 40 km in northern Honshu.

Introduction

Convolution appears in nearly every facet of geophysics. A typical situation is where some observed function results from the convolution of two functions, with one function "reasonably well-known" and the other function unknown. In many applications, the observed function is a time series, e.g., a seismogram. Since convolution is a linear operation, deconvolution of the unknown function is a linear inverse problem. Unfortunately, inversion of the convolution integral is fraught with problems (see e.g., Parker, 1977).

For the particular application of deconvolution of earthquake source time functions from body wave seismograms, problems arise since the "reasonably well-known" function (the earthquake Green's function) contains only a certain band of frequencies, and also possesses spectral holes within this passband (see Ruff and Kanamori, 1983). To obtain a more reliable source time function for a particular earthquake, one could deconvolve several seismograms to produce multiple estimates of the source time function, or even better, simultaneously invert several seismograms for a single "best" source time function. This latter procedure is particularly appropriate for small to intermediate size earthquakes (up to magnitude 7).

Unfortunately, we encounter another problem when simultaneously inverting long period *P* and *S* waveforms: while the waveshapes can be matched extremely well, unexplained absolute amplitude variations of a factor of two or more degrade the significance of the solution. Recognition of this amplitude scatter began as early as the original development of the magnitude scales by Richter and Gutenberg, who also established the practice of using log averages for amplitude data. Although we now have better theories and computational schemes to account for earthquake radiation patterns and the subsequent wave propagation effects, the amplitude scatter remains. In fact, many seismologists will simply scale the seismograms in an *ad hoc* fashion to produce the best match when using long period *P* and/or *S* waves. Note that amplitude scatter is a special type of "noise"; it does not conform to the typical assumption of normally distributed, uncorrelated, additive noise. It is time to formally acknowledge and accommodate the scaling factor incompatibility when inverting a set of waveforms. Omnilinear inversion achieves this goal.

Source Time Function Deconvolution

Long period teleseismic *P* and *S* waves from a shallow (depth<70 km) intermediate size (magnitude of 6 to 7) earthquake are strongly affected by the focal mechanism, depth, and source time history of the event (see Langston and Helmberger, 1975). In many instances, a good estimate for the focal mechanism of an intermediate size earthquake is available (e.g., Harvard centroid moment tensor mechanisms). Thus, all the earthquake parameters are well-known except for depth and source time function. For a given depth, a seismogram at a particular station results from the convolution of the effective point source Green's function, $g(t)$, and the source time function, $f(t)$, i.e., $s(t)=g(t)*f(t)$. The source time function can be deconvolved from a single seismogram.

Now suppose that a set of n seismograms, $s_1(t),...,s_n(t)$, are to be inverted for the overall best source time function. There is a different Green's function for each seismogram: $g_1(t),...,g_n(t)$. To proceed, discretize the convolution integral with each seismogram now given as: $G_if=s_i$, where the column vector s_i is the discretized i^{th} seismogram, G_i is a matrix that contains the i^{th} Green's function, and the unknown column vector f is the discretized source time function. With multiple seismograms providing multiple estimates of the source time function, the combined quasi-overdetermined problem is $Gf=d$, where G and d are defined as: $G^T=[G_1^T, G_2^T, \ldots, G_n^T]$ and $d^T=[s_1^T, s_2^T, \ldots, s_n^T]$, the transposed equations are used above to conserve space. Given some estimate for f, say f_E, the error vector will be the difference between the observed and synthetic seismograms: $e=d-Gf_E$. Statistical statements concerning the "noise" in d can be used to determine f_E. In the standard least-squares statement, define the squared length of the error vector to be: $\psi=e^Te$, and find the minimum of ψ with respect to the components of f_E. Thus a suitable f_E can be found for a given depth. Since focal depth is a single parameter that enters g(t) in a complicated manner, the typical procedure is to invert for the best f_E at a number of trial depths, and then choose the depth that produces the overall minimum value for ψ as the best focal depth. We are now ready to enlarge the scope of the inversion problem.

Paper number 89GL01509.
0094-8276/89/89GL-01509$03.00

Omnilinear Inversion

The omnilinear equations differ from the above "standard" linear equations in that the seismogram scale factors ($a_1, a_2, \ldots, a_n$) are explicitly included as factors in the data vector: $[Gf]^T=[a_1 s_1^T, a_2 s_2^T, \ldots, a_n s_n^T]$. The key step is now simply rewriting the data vector in its column vector form as: Sa, where S is a matrix with n column vectors, the i^{th} column vector contains s_i and zeroes elsewhere; and the a vector contains the n scale factors. If all components of a are equal to one, then Sa is the "standard" data vector. As a brief digression, the term "omnilinear" makes the distinction between our statistical estimation problem and the analysis of a homogeneous linear system. In particular, omnilinear inversion can be viewed as a variation of Hotelling's (1936) canonical correlation analysis.

The error vector for omnilinear equations is then: $e=Sa-Gf_E$, where f_E is again the source time function estimate. The least-squares estimate for f_E is: $f_E=(G^TG)^{-1}G^Td=(G^TG)^{-1}G^TSa$. With the substitution of the latter expression for f_E into the error vector, e now depends on just a. Thus the squared length of the error vector, $\psi=e^Te$, can now be minimized with respect to the components of a. There is a crucial difference between this minimization problem and that for "standard" linear inversion: ψ is always identically zero if all components of a are zero. To exclude this trivial solution, the above minimization problem must be solved with an additional constraint equation for a. For the case of amplitude scatter in waveform inversion, the *a priori* statistical expectation (see earlier discussion) is that the *a*'s follow a log-normal distribution. In other words, it is equally likely that the amplitudes are 50% larger or 50% smaller than predicted. The log-normal expectation is represented by the product of the *a*'s set equal to one: $\Pi_i a_i=1$. While other constraint equations are appropriate for different physical problems, there is no space to present them here. In the following applications, error will be measured by the scalar quantity: $e=\sqrt{(e^Te/d^Td)}$, hence *e* is the ratio of the error vector length to data vector length.

The omnilinear inverse problem for f_E and a is thus: with $f_E=(G^TG)^{-1}G^TSa$, minimize $\psi=e^Te=(Sa-Gf_E)^T(Sa-Gf_E)$ with respect to the components of a, subject to the constraint that $\Pi_i a_i=1$. After a is found, f_E is completely specified. It is now important to assess the performance of omnilinear inversion--in short, does it work?

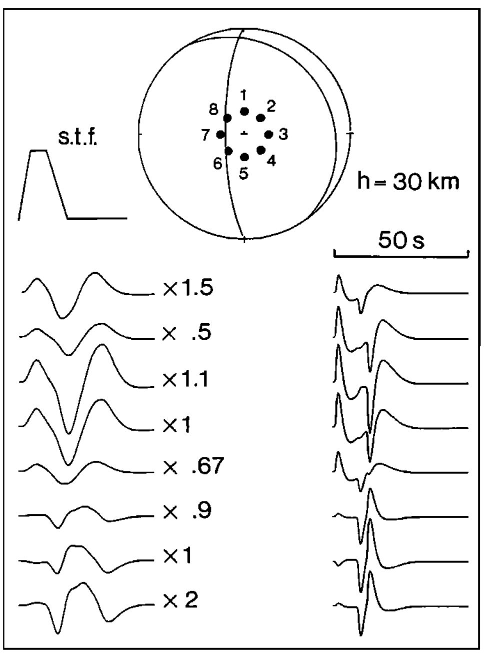

Fig. 1. Synthetic event experiment with amplitude scatter. Station locations for the eight *P* waves are shown on the focal sphere with the oblique underthrusting mechanism. Green's functions (column at right) are ordered top to bottom for stations #1 through #8, and are constructed for the WWSSN-LP instrument and a focal depth of 30 km. Green's functions are convolved with the trapezoidal source time function (s.t.f.) and the resultant seismograms are scaled with arbitrary scale factors, listed next to the final "observed" seismograms (column at left).

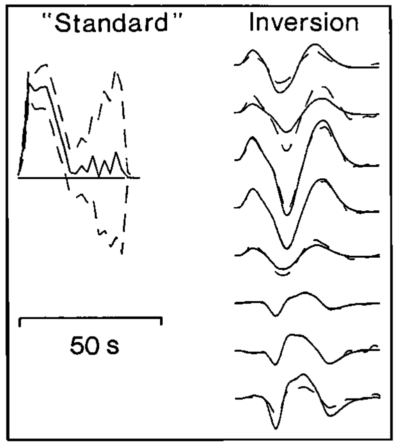

Fig. 2. Source time function and match to seismograms for "standard" linear inversion at a focal depth of 30 km. The eight "observed" seismograms are plotted as the solid traces, while the best-match synthetic seismograms are the dashed traces. The source time function and standard deviation are plotted on the left as the solid and dashed traces, respectively. Seismic moment is overestimated by 20%.

Omnilinear Inversion of Synthetic Data

Synthetic *P* waves are generated for a typical underthrusting mechanism at a depth of 30 km (V_P is 6.7 km/s and V_P/V_S is $\sqrt{3}$) and a simple trapezoidal time function of 18 s duration (see

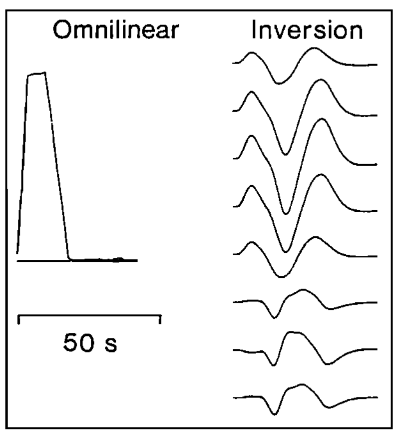

Fig. 3. Source time function and match to seismograms for omnilinear inversion at a focal depth of 30 km. The rescaled "observed" seismograms (solid traces) and the synthetic seismograms (dashed traces) exactly match at this depth. Omnilinear inversion recovers the correct source time function, shown at left.

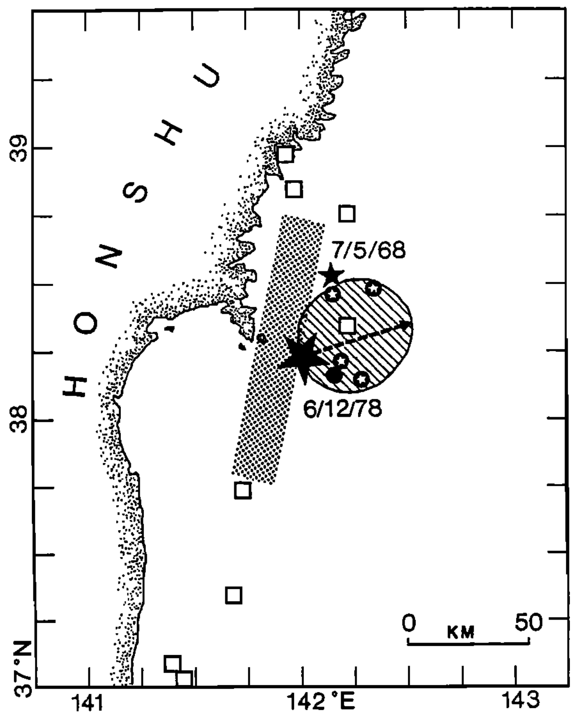

Fig. 4. Seismological setting of the July 5, 1968 northern Honshu (Japan) earthquake (adapted from Tichelaar and Ruff, 1988). The Pacific plate subducts to the west beneath Honshu. The 6/12/78 Miyagi-Oki mainshock epicenter is plotted as the large star, its teleseismic one-day aftershocks are the open dots, enclosed by the hachured region. The bold broken line depicts the mainshock rupture direction and extent. Other epicenters are: foreshock of the 1978 event (solid dot); other large underthrusting events from 1962 to present (open boxes), including the 7/5/68 event (star). The wide stipled bar represents the transition between a coupled and uncoupled plate interface.

Figure 1). To simulate amplitude scatter, the synthetic seismograms are then multiplied by the scale factors shown in Figure 1. To now determine the best depth and source time function, the seismograms are inverted for seven trial depths between 10 and 50 km. All other parameters are correctly specified. For each trial depth, both "standard" inversion and omnilinear inversion are applied to the seismograms. Omnilinear inversion matches the data exactly only at the correct depth of 30 km, while "standard" inversion produces an error curve with a weak minimum for depths from 25 to 35 km. The mismatch between "observed" and synthetic seismograms for "standard" inversion can be seen in Figure 2. For linear inverse problems, the *a posteri* variance is easily mapped into the model covariance matrix, and the diagonal elements can then be used to plot the standard deviation of the source time function (see Figure 2). Given this level of uncertainty in the time function, it is quite risky to base conclusions on subtle details of the time function.

Omnilinear inversion error is zero at the correct depth of 30 km as the correct scale factors are found. This is demonstrated graphically in Figure 3 where the "observed" seismograms are perfectly rescaled to eradicate data incompatibility. Consequently, the standard deviation of the source time function tends to zero; not perfectly recovering the source time function comes from poor model resolution. Although the error will never be reduced to zero with real seismograms, omnilinear inversion always serves to reduce data incompatibility and thereby improve model reliability. The robustness of omnilinear inversion makes scale factor determination quite reliable. But does omnilinear inversion work for real seismograms?

TABLE 1. WWSSN station codes with epicentral distance, Δ, and azimuth, φ, (deg.) from 5 JUL 68 Honshu event.

	COL	ALQ	CTA	NDI	AAE	JER	NOR
Δ	48	83	58	54	95	83	60
φ	32	50	176	280	285	305	357

The July 5, 1968 Northern Honshu Earthquake

Tichelaar and Ruff (1988) studied the 1978 Miyagi-Oki earthquake (M_S 7.5) to determine the downdip edge of seismic coupling in the northern Honshu (Japan) subduction zone. They concluded that the mainshock rupture extended no deeper than 40 km. Determination of rupture extent for large earthquakes is difficult due to the long duration of the source time function. Smaller interplate events that occur at the downdip edge of a mainshock rupture provide the opportunity to better define the depth of the seismogenic zone. The earthquake of July 5, 1968

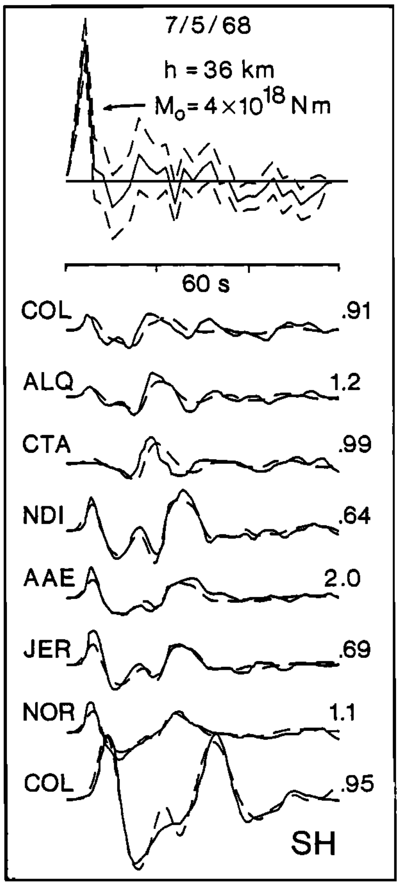

Fig. 5. Omnilinear inversion for source time function and scale factors at the best focal depth of 36 km. The rescaled seismograms are plotted as solid traces with best-fit synthetics as dashed traces, the omnilinear scale factors are listed on the right. The source time function and its standard deviation are plotted as the solid and dashed traces at top.

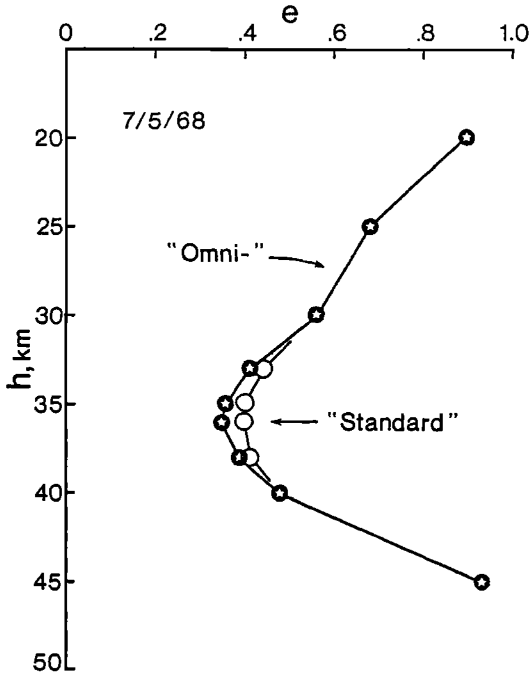

Fig. 6. Error parameter as a function of focal depth for "standard" and "omni-" linear inversion of the body waves for source time function. For this data set, omnilinear inversion significantly reduces the error only in the depth range of 33 to 38 km, with the best match at 36 km.

(M_S 6.6, M_{JMA} 6.4, ISC origin time and hypocenter, 11:28:13.0, 38.54°N 142.14°E, depth 44 km) occurs adjacent to the downdip edge of the Miyagi-Oki mainshock (see Figure 4).

The first-motion mechanism for the July 5, 1968 event is well-constrained and compatible with the 1978 mainshock mechanism (ϕ=190°, δ=20°, λ=76°, Seno et al., 1980). To demonstrate omnilinear inversion, seven P waves and one SH wave are selected (see Table 1 and Fig. 5). The procedure is the same as for the synthetic test (V_P=6.7 km/s, t^*_P=1 s, t^*_S=4 s); the error curves for "standard" and omnilinear inversion are plotted in Figure 6. The best focal depth is 36 km, and omnilinear inversion reduces e from 0.40 to 0.35 at this depth. Figure 5 shows the omnilinear solution at the best depth. Note that the diffracted P wave at AAE is scaled up by a factor of two. The SH wave amplitude at COL is quite compatible with the P wave amplitudes. Omnilinear inversion enhances the error minimum at 36 km to better resolve the focal depth, thus supporting the earlier conclusion of Tichelaar and Ruff (1988).

Conclusions

The future of waveform inversion studies is to extract more detailed, yet more reliable, quantitative information about both earthquakes and earth structure. A major source of incompatibility between observed and synthetic waveforms is amplitude scatter. Omnilinear inversion explicitly includes and determines these seismogram scale factors. Future investigations shall tell whether these scale factors are useful for earth structure studies. Application of omnilinear inversion to P and SH waves from the northern Honshu underthrusting earthquake of July 5, 1968 confirms that the downdip edge of the seismically coupled zone extends no deeper than 40 km in this region.

Acknowledgements. Thanks to Bart Tichelaar, Susan Schwartz, Peter Shaw, Jiajun Zhang, and an anonymous reviewer for their helpful comments. Thanks to Kathy Sharpe at UW for production help. Earthquake studies at Univ. of Michigan are supported by the National Science Foundation (EAR8720935 to L.J.R.).

References

Hotelling, H., Relation between two sets of variates, *Biometrika, 28,* 321-377, 1936.

Langston, C.A., and D.V. Helmberger, A procedure for modeling shallow dislocation sources; *Geophys. J. R. Astron. Soc., 42,* 117-130, 1975.

Parker, R.L., Understanding inverse theory, *Ann. Rev. Earth Planet. Sci., 5,* 35-64, 1977.

Ruff, L.J., and H. Kanamori, The rupture process and asperity distribution of three great earthquakes from long-period diffracted P-waves, *Phys. Earth Planet. Int., 31,* 202-230, 1983.

Seno, T., K. Shimazaki, P. Sommerville, K. Sudo, and T. Eguchi, Rupture process of the Miyagi-Oki, Japan, earthquake of June 12, 1978, *Phys. Earth Planet. Int., 23,* 39-61, 1980.

Tichelaar, B.W., and L.J. Ruff, Rupture extent of the 1978 Miyagi-Oki, Japan, earthquake and seismic coupling in the northern Honshu subduction zone, *Geophys. Res. Lett., 15,* 1219-1222, 1988.

L. Ruff, Department of Geological Sciences, University of Michigan, Ann Arbor, MI 48109.

(Received July 21, 1989;
accepted July 21, 1989)